

## Template Structure at the Silicon/Amorphous-Silicide Interface

P. A. Bennett, M. Y. Lee, and P. Yang

*Department of Physics and Astronomy, Arizona State University, Box 871504, Tempe, Arizona 85287-1504*

R. Schuster,\* P. J. Eng,<sup>†</sup> and I. K. Robinson

*Physics Department, University of Illinois, Urbana, Illinois 61801*

(Received 15 May 1995)

Surface x-ray diffraction was used to monitor the reaction of Ni on Si(111) at room temperature. Intensity oscillations during deposition signify that a layerwise reaction occurs for the first 30 Å of metal deposited, forming a silicide overlayer with stoichiometry Ni<sub>2</sub>Si. Structural analysis of the interfacial layers detects an epitaxial and commensurate phase, Ni<sub>2</sub>Si- $\theta$ , with long range order imposed by the substrate but with very large local atomic displacements. This epitaxial structure remains at the interface as amorphous silicide forms above it.

PACS numbers: 68.35.Bs, 68.55.Bd, 68.55.Eg, 68.55.Jk

Silicide overlayers on Si have been widely studied, both because of their practical importance in the fabrication of electronic devices and because they can form atomically perfect, metal-semiconductor interfaces [1,2]. Much effort has focused on the topic of the initial stages of silicide reactions (low temperature and/or low coverage) with the aim of identifying, understanding, and eventually controlling the overlayer growth [3–6]. Indeed, “template” methods of growth exist, by which the atomic and electronic structure of thick overlayers can be usefully modified by manipulating monolayer template layers in the initial stage of growth [7,8]. On a more general level, this topic is part of the larger issues of “first-formed phase” and “solid state amorphization reactions,” about which many questions remain [9–11].

The above issues all involve the central question of the evolving structure at the buried interface between substrate and overlayer during a solid phase reaction. This is an experimentally challenging question for which x-ray diffraction is ideally (perhaps uniquely) suited, both because the penetrating radiation can reach the buried interface and because the diffraction process allows extraction of relatively small signals from monolayer commensurate structures lying under amorphous overlayers.

We have chosen the Ni/Si(111) system for this study, because it forms a commensurate epitaxial silicide and because of its thorough background in the literature. As with all silicides, the question of which phase forms first during low temperature deposition remains controversial, with evidence for Ni<sub>2</sub>Si, NiSi, or NiSi<sub>2</sub> as well as “glassy” phases [5,12–14]. Ion scattering measurements show that the stoichiometry of the overlayer is Ni:Si = 2:1, at least for coverages above 3 monolayers (ML). In some cases a progression of stoichiometries from 1:2 in the first monolayers to pure Ni at higher coverage has been reported [15]. A genuine amorphous film has been observed in multilayer structures [11]. A template effect is particularly notable in the context of the introduction. Namely, it is

found that the growth of epitaxial NiSi<sub>2</sub> on Si(111) by low temperature co-deposition of Ni and Si is optimized by a precoat of 3 Å of Ni [7]. From this it is inferred that the template layer (and first-formed phase) is NiSi<sub>2</sub>.

In this paper we show that Ni<sub>2</sub>Si is the first and only silicide to form during low temperature deposition of Ni on Si(111), in agreement with ion scattering results at higher coverage. Furthermore, the first several layers are epitaxial and commensurate with the substrate, while subsequent layers are not. The overlayer possesses long range order, which is imposed by the substrate; however, the local atomic positions are highly disordered. We suggest that this feature may be characteristic of the crystal-amorphous interface.

Diffraction measurements were made on beamline X16A at the National Synchrotron Light Source (NSLS), Brookhaven, NY. This station features a 5-circle diffractometer carrying a fully bakeable UHV system [16]. For this paper we choose a hexagonal unit cell defined as  $(1,0,0)_{\text{hex}} = 1/3(4, 2, 2)_{\text{cubic}}$  and  $(0,0,3)_{\text{hex}} = (1,1,1)_{\text{cubic}}$ . This coordinate choice maintains a pure index  $L$  for the out-of-plane direction, while indices  $h$  and  $k$  span the in-plane directions. Crystal truncation rod (CTR) profiles were measured by integrating a set of rocking curves at various  $L$  values along a given rod. Structure factors were obtained from integrated intensities after standard corrections for illuminated area, Lorentz factor, and polarization. Equivalent rods were averaged assuming  $p3m1$  symmetry (imposed by the substrate), and typically agreed to within 15% at each  $L$  value.

The Si(111) substrates were cleaned by light sputtering and annealing in UHV to 1500 K, which produced a  $7 \times 7$  reconstructed surface. Ni was deposited by sublimation from a 0.020 in. diameter high purity wire. Samples were mounted in contact with large Ta blocks which helped hold the temperature rise to less than 10 °C during deposition. Ni coverage was calibrated *in situ* with a quartz balance, and *ex situ* by ion scattering giving an

absolute accuracy of 15%. Values are given here in terms of ML where  $1 \text{ ML} = 7.8 \times 10^{-14} \text{ cm}^{-2}$ .

In Fig. 1 we show the CRT profiles for the (1,0) and (2,0) rods, following deposition of 3.2 ML of Ni at room temperature. The dotted line shows the calculated (1,0) CTR profile for an ideal bulk-terminated Si(111) surface, with Bragg reflections at  $L = -2$  (forbidden),  $+1$ , and  $+4$ . Both measured rods clearly show hexagonal symmetry with additional features near  $L = \pm 2$  and  $\pm 4$ . These features are most notable on the (1,0) rod at  $L = -4$  and  $-2$ , where the substrate contribution is small, but also noticeable at  $L = +2$  and  $\pm 4$ , where they mix (coherently) with the substrate amplitude. Since these features appear on a nonspecular rod ( $Q_{\text{parallel}} \neq 0$ ), they necessarily arise from a coherent and commensurate epitaxial phase. Candidate structures in the Ni-Si binary system include  $\text{Ni}_2\text{Si}-\delta$ ,  $\text{Ni}_2\text{Si}-\theta$ , NiSi, and  $\text{NiSi}_2$ , all of which are reported to grow epitaxially on Si(111) to various degrees [17–20]. Of these, only  $\text{Ni}_2\text{Si}-\theta$  has the hexagonal symmetry observed in our experiment, as well as unit cell dimensions that match the data. *B*-type  $\text{NiSi}_2$ , in particular, is excluded, since it would produce a large peak at  $\mathbf{Q} = (1, 0, -1)$ , which is not present in the data. Other, more exotic possibilities to consider are isomorphous analogs to the recently reported diamond cubic  $\text{CoSi}_2$  [21] and bcc  $\text{CoSi}$  [22] structures. Both are excluded on the basis of symmetry and/or peak positions along the rods.

We confirm and quantify the identification of the epitaxial structure by making explicit calculations of the CTR profiles. Thus, the amplitude scattered from the combined system of substrate plus silicide overlayers

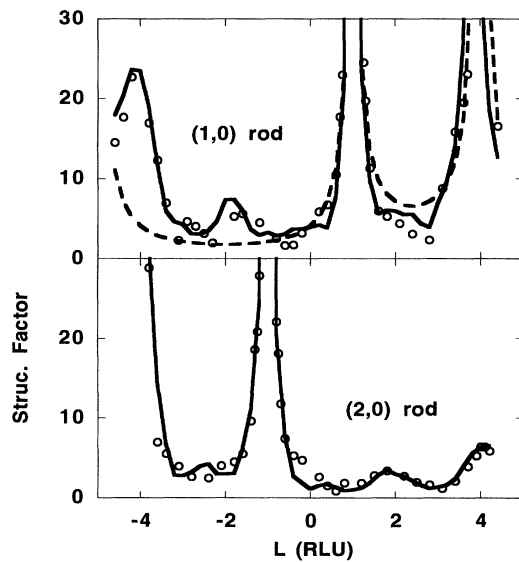


FIG. 1. (1,0) and (2,0) rod profiles following deposition of 3.2 ML Ni. Lines show calculation for bulk-terminated Si(111) (dashed) and for model  $\text{Ni}_2\text{Si}-\theta$  overlayer (solid).

may be written as

$$A(\mathbf{Q}) = F_b \sum_{n=1}^{\infty} e^{-in\mathbf{Q}\cdot\mathbf{R}} + W_{\text{Si}} F_b + e^{i\mathbf{Q}\cdot\mathbf{R}_{\text{ol}}} \sum_{j=1}^N W_j \sum_{m=1}^M F_{j,m} e^{i\mathbf{Q}\cdot\mathbf{r}_{j,m}}, \quad (1)$$

where  $F_b$  and  $F_{j,m}$  are complex structure factor amplitudes (with assumed summation over all unit cells in the lateral direction) for bilayers of silicon and for the  $m$ th atom in the unit cell of the  $j$ th layer of silicide,  $W_{\text{Si}}$  and  $W_j$  are occupancy (less than unity) plus Debye-Waller weighting factors for silicon bilayers and silicide overlayers,  $\mathbf{R} (= 1/3, 2/3, 1/3)a_0$  is the translation vector between silicon bilayers,  $\mathbf{r}_{j,m}$  are the unit cell coordinates of silicide atoms, and  $\mathbf{R}_{\text{ol}}$  is a registration vector for the entire overlayer relative to the substrate. Overlayer atoms are assumed to occupy lattice sites at random, so the scattered intensity is confined to perfectly narrow rods. In fitting a model structure, the only free parameters are the layer weights  $W_j$  and  $W_{\text{Si}}$ , the registration vector  $\mathbf{R}_{\text{ol}}$ , and a layer spacing along the surface normal (contained in  $\mathbf{r}_{j,m}$ ). An overall scale factor is determined by matching the CTRs near the bulk Si Bragg peaks, and the coordinates  $\mathbf{r}_{j,m}$  are taken from known bulk silicide values, after allowing a uniform strain to match the substrate mesh.

The dashed line in Fig. 1 shows  $|A(\mathbf{Q})|$  for the substrate CTR alone [first term in Eq. (1)]. The solid lines show  $|A(\mathbf{Q})|$  for a model  $\text{Ni}_2\text{Si}-\theta$  structure. In the fitting, we constrained the many individual  $W_j$  to be equal within a unit layer of  $\text{Ni}_2\text{Si}$  (containing 4 Ni and 2 Si atoms per substrate unit mesh), but allowed separate weights ( $W_a, W_b, W_c$ , etc.) for each such unit layer. Thus the total number of Ni atoms in the overlayer (in ML units) was parametrized as  $N_{\text{tot}} = 4W_Q(W_a + W_b + W_c)$ . The fit proceeded by manual adjustment of parameters and chi square values, aided by visual inspection. We first concentrated on regions of the rods where the silicide peaks are large and the substrate contribution is small in order to decouple their interference. Thus the heights of the silicide features near  $\mathbf{Q} = (1, 0, -4)$  and  $(2, 0, 4)$  essentially determine  $N_{\text{tot}}$ , while their widths determine the silicide “roughness,” specified by the values of  $W_a, W_b, W_c$ , and their positions determine the layer spacing. Finally, we adjusted  $\mathbf{R}_{\text{ol}}$  to optimize  $|A(\mathbf{Q})|$  in the regions where the substrate and overlayer contributions are similar in magnitude.

A reasonable fit is obtained for all four of the inequivalent rods measured  $\{(1,0), (2,0), (1,1), \text{ and } (3,0)\}$ , using the same values of all parameters *except*  $W_Q$  (see below). The layer spacing in the silicide is found to contract by 5%, which is somewhat more than expected from the 1% lateral expansion required to match the substrate. Returning to the  $W_Q$  values, we note that they follow an exponential trend given by  $W_Q = W_0 e^{-B|Q|^2}$ , as shown in Fig. 2. Here,  $|Q| = \sin(\theta)/\lambda$  is determined by the rod index and value of  $L$  at the largest silicide peak on the rod.

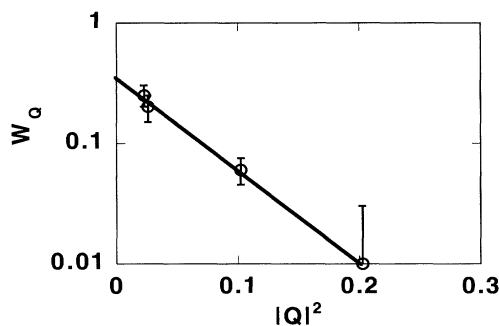


FIG. 2.  $Q$  dependence of weight factors  $W_Q$ , determined from fitting model calculations with data for (1,0), (1,1), (2,0), and (3,0) rods.

The error bars represent  $W_Q$  values for which the calculated curve lies wholly above or below two-thirds of the data points in the silicide peaks. This functional dependence, and the fact that the rods remain sharp and commensurate, suggests a static disorder that mimics thermal disorder, by which we mean that atomic displacements about well-defined lattice positions occur. From this plot we determine a value of  $W_0 = 0.33$  ML for the “rigid lattice extrapolation” to  $Q = 0$ , and a value of  $B = 17 \text{ \AA}^2$ . We could not cool the sample to prove that the  $W_Q$  are independent of temperature, but infer this from the extremely large value of  $B$  compared with typical thermal values of  $B \sim 1$ . The large static disorder in the epitaxial layer likely explains why epitaxy was not detected in earlier ion scattering experiments [23]. The fact that  $W_0 < 1$  means that island structures are formed. Islanding is also directly signified by the width  $\Delta L$  of silicide features on the rod scans, which corresponds to a film thickness of 9  $\text{\AA}$ , about twice that expected for a uniform overlayer.

The total amount of Ni found in the epitaxial silicide peak is given by  $4W_0(1 + 0.6 + 0.3) = 2.5$  ML, which compares with the amount of Ni deposited, 3.2 ML. These agree within the uncertainties, showing that  $\text{Ni}_2\text{Si}-\theta$  is the only phase formed at this coverage and temperature.

Next we discuss the coverage dependence of the reaction. In Fig. 3 we show the variation of diffracted intensity during deposition of Ni at room temperature. In the top panel we show the behavior at  $Q = (1,0,2.5)$ , which is chosen such that the scattering from successive Si(111) bilayers is  $\pi$  out of phase. This makes the intensity maximally sensitive to changes in the surface layers. Also note that the contribution from the epitaxial silicide is small at this value of  $Q$ . The intensity shows four distinct maxima spaced by approximately 5 ML. The oscillating behavior is caused by a layerwise etching of the Si(111) substrate, as was found also for Pd/Si(111) [24]. That is, the silicon-silicide interface remains “sharp” and alternates between complete and half-filled Si(111) bilayers. The period of oscillation determines the stoichiometry of the silicide formed in this reaction

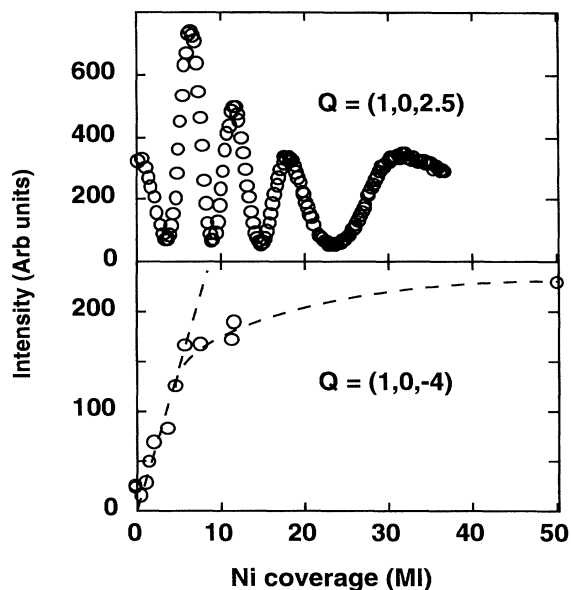


FIG. 3. Intensity oscillations during deposition observed at  $Q = (1,0,2.5)$ , where the silicide contribution is negligible (upper panel). Growth of epitaxial  $\text{Ni}_2\text{Si}-\theta$  observed at  $Q = (1,0,-4)$ , where the silicide contribution dominates (lower panel).

as Ni:Si = 5:2, assuming that Si bilayers are consumed in the reaction as commonly occurs on Si(111). This stoichiometry agrees with that of the epitaxial silicide  $\text{Ni}_2\text{Si}-\theta$ , within the uncertainty of flux calibration. We note that the reaction continues up to about 30 ML, where it then slows dramatically, and asymptotically stops.

In the bottom panel we show the amount of epitaxial  $\text{Ni}_2\text{Si}-\theta$  formed during the reaction, obtained in a separate experiment as the integrated intensity measured at  $Q = (1,0,-4)$ . At this value of  $Q$ , the silicide amplitude is a maximum and the substrate amplitude is negligible, so the intensity does not oscillate. The dotted line shows the value expected if all the deposited metal forms epitaxial  $\text{Ni}_2\text{Si}-\theta$ . This does indeed occur up to about 6 ML, where the epitaxial growth stops rather suddenly, even though silicon continues to be consumed at the same rate (as indicated by the intensity oscillations), presumably forming nonepitaxial  $\text{Ni}_2\text{Si}$ . This additional silicide contributes no sharp diffraction peaks anywhere and is presumed to be amorphous [11,23].

Upon annealing, the overlayer evolves in two distinct steps. First a 7  $\text{\AA}$  film first converts to well-ordered  $\text{Ni}_2\text{Si}-\theta$  at about 100  $^\circ\text{C}$ , and the strong variation of  $W$  with  $|Q|$  goes away. This confirms the idea of large static disorder in the as-deposited overlayer. Above 200  $^\circ\text{C}$ ,  $B$ -type  $\text{NiSi}_2$  is formed.

Our results shed light on several long-standing issues in the Ni/Si(111) system. Regarding the “template” effect mentioned in the introduction, clearly the islanded  $\text{Ni}_2\text{Si}-$

$\theta$  layer formed by 3 Å deposition of Ni on Si(111) is not simply a structural template for epitaxial NiSi<sub>2</sub>. The islands of Ni<sub>2</sub>Si- $\theta$  do not even form a homogeneous or flat surface on which to grow. Rather, we suggest that the template effect involves a more subtle, chemical mechanism such as passivation of the original Si surface. Our results also reopen the question of the thickness-induced switch from *B*-type to *A*-type NiSi<sub>2</sub> growth first reported by Tung, Gibson, and Poate [8]. Our finding that epitaxial Ni<sub>2</sub>Si- $\theta$  forms directly at the lowest coverages is at variance with an earlier report that stated that this phase forms only in thicker films during annealing and leads directly to *A*-type NiSi<sub>2</sub>, suppressing formation of *B*-type NiSi<sub>2</sub> [25].

Our results may also shed light on epitaxial growth in a broader sense. It is interesting that the epitaxial growth of Ni<sub>2</sub>Si- $\theta$  stops at nearly the coverage of the first oscillation maximum. Due to islanding, the areal coverage is still far from unity, so “bare Si” is still available. This suggests that nucleation at the essentially flat interface, rather than access to bare substrate, limits the epitaxial growth. Epitaxy may also be limited by the buildup of large amounts of strain in the epitaxial islands, as suggested by the Debye-Waller plot in Fig. 2. Indeed, one can formally interpret amorphization in terms of static atomic displacements of this magnitude [26]. We speculate that this behavior may be responsible for the “critical epitaxial thickness” observed in the homoepitaxial system Si/Si(100) [27]. Unfortunately, it would be difficult to directly observe this effect using x rays since the overlayer scattering is not readily distinguishable from the substrate scattering, unlike the Ni/Si(111) case.

This work was supported in part by NSF Grants No. DMR92-21201 and No. DMR93-15691. The NSLS is supported by the DOE under Grant DE-AC02-76CH00016.

\*Present address: Abt. Phys. Chemie, Fritz-Haber Institute, Faradayweg 4-6, D14195 Berlin.

†Present address: CARS, University of Chicago, Chicago, IL 60637.

[1] A. H. Reader, A. H. vanOmmen, P. J. W. Weijs, R. A. M. Wolters, and D. J. Oostra, *Rep. Prog. Phys.* **56**, 1397 (1992).

- [2] M. A. Nicolet and S. S. Lau, in *VLSL Microstructure Science*, edited by N. G. Einspruch and G. B. Larrabee (Academic, New York, 1983), p. 330.
- [3] A. Hiraki, *Surf. Sci. Rep.* **3**, 357 (1984).
- [4] T. L. Lee and L. J. Chen, *J. Appl. Phys.* **75**, 2007 (1994).
- [5] J. R. Butler and P. A. Bennett, *Mater. Res. Soc. Symp. Proc.* **159**, 159 (1990).
- [6] P. A. Bennett, D. G. Cahill, and M. Copel, *Phys. Rev. Lett.* **73**, 452 (1994).
- [7] R. T. Tung and F. Schrey, *Appl. Phys. Lett.* **55**, 256 (1989).
- [8] R. T. Tung, J. M. Gibson, and J. M. Poate, *Phys. Rev. Lett.* **50**, 429 (1983).
- [9] R. M. Walser and R. W. Bene, *Appl. Phys. Lett.* **28**, 624 (1976).
- [10] M. Ronay, *Appl. Phys. Lett.* **42**, 577 (1983).
- [11] K. Holloway, R. Sinclair, and M. Nathan, *J. Vac. Sci. Technol. A* **7**, 1479 (1989).
- [12] P. A. Bennett, J. R. Butler, and X. Tong, *Mater. Res. Soc. Symp. Proc.* **148**, 61 (1989).
- [13] P. A. Bennett, J. R. Butler, and X. Tong, *J. Vac. Sci. Technol. A* **7**, 2174 (1989).
- [14] H. vonKanel, *Mater. Sci. Rep.* **8**, 193 (1992).
- [15] P. J. Grunthaner, F. J. Grunthaner, and J. W. Mayer, *J. Vac. Sci. Technol.* **17**, 924 (1980).
- [16] P. H. Fuoss and I. K. Robinson, *Nucl. Instrum. Methods* **222**, 171 (1984).
- [17] J. Foll, P. S. Ho, and K. N. Tu, *Philos. Mag. A* **45**, 31 (1982).
- [18] F. d’Heurle, C. S. Petersson, J. E. E. Baglin, S. J. LaPlaca, and C. Y. Wong, *J. Appl. Phys.* **55**, 4208 (1984).
- [19] P. A. Bennett, X. Tong, and J. R. Butler, *J. Vac. Sci. Technol. B* **6**, 1336 (1988).
- [20] J. M. Gibson and J. L. Batstone, *Surf. Sci.* **208**, 317 (1989).
- [21] S. L. Zhang, J. Cardenas, F. M. d’Heurle, B. G. Svensson, and C. S. Petersson, *Appl. Phys. Lett.* **66**, 58 (1995).
- [22] H. vonKanel, C. Schwarz, S. Goncalves-Conto, E. Muller, L. Miglio, F. Tavazza, and G. Malegori, *Phys. Rev. Lett.* **74**, 1163 (1995).
- [23] E. J. vanLoenen, J. F. vanderVeen, and F. K. LeGoues, *Surf. Sci.* **157**, 1 (1985).
- [24] P. A. Bennett, B. Devries, I. K. Robinson, and P. J. Eng, *Phys. Rev. Lett.* **69**, 2539 (1992).
- [25] J. M. Gibson, J. L. Batstone, R. T. Tung, and F. C. Unterwald, *Phys. Rev. Lett.* **60**, 1158 (1988).
- [26] N. Q. Lam and P. R. Okamoto, *Mater. Res. Soc. Symp. Proc. Bull.*, July 1994, p. 41.
- [27] D. J. Eaglesham, H. J. Gossman, and M. Cerullo, *Phys. Rev. Lett.* **65**, 1227 (1990).